

Article

The Depositional Environments in the Cilento Offshore (Southern Tyrrhenian Sea, Italy) Based on Marine Geological Data

Gemma Aiello ^{1,*} and Mauro Caccavale ^{1,2}

¹ Istituto di Scienze Marine (ISMAR), Consiglio Nazionale delle Ricerche (CNR), 80133 Napoli, Italy; mauro.caccavale@cnr.it

² Istituto Nazionale di Geofisica e Vulcanologia, Osservatorio Vesuviano, 80133 Napoli, Italy

* Correspondence: gemma.aiello@cnr.it

Abstract: The depositional environments offshore of the Cilento Promontory have been reconstructed based on the geological studies performed in the frame of the marine geological mapping of the geological sheet n. 502 “Agropoli”. The littoral environment (toe-of-coastal cliff deposits and submerged beach deposits), the inner continental shelf environment (inner shelf deposits and bioclastic deposits), the outer continental shelf environment (outer shelf deposits and bioclastic deposits), the lowstand system tract and the Pleistocene relict marine units have been singled out. The littoral, inner shelf and outer shelf environments have been interpreted as the highstand system tract of the Late Quaternary depositional sequence. This sequence overlies the Cenozoic substratum (ssi unit), composed of Cenozoic siliciclastic rocks, genetically related with the Cilento Flysch. On the inner shelf four main seismo-stratigraphic units, overlying the undifferentiated acoustic basement have been recognized based on the geological interpretation of seismic profiles. On the outer shelf, palimpsest deposits of emerged to submerged beach and forming elongated dunes have been recognized on sub-bottom profiles and calibrated with gravity core data collected in previous papers. The sedimentological analysis of sea bottom samples has shown the occurrence of several grain sizes occurring in this portion of the Cilento offshore.

Keywords: littoral deposits; continental shelf deposits; palimpsest deposits; marine geological maps; Cilento Promontory; Southern Italy

Citation: Aiello, G.; Caccavale, M. The Depositional Environments in the Cilento Offshore (Southern Tyrrhenian Sea, Italy) Based on Marine Geological Data. *J. Mar. Sci. Eng.* **2021**, *9*, 1083. <https://doi.org/10.3390/jmse9101083>

Academic Editor: Antoni Calafat

Received: 5 September 2021

Accepted: 29 September 2021

Published: 4 October 2021

Publisher’s Note: MDPI stays neutral with regard to jurisdictional claims in published maps and institutional affiliations.



Copyright: © 2021 by the authors. Licensee MDPI, Basel, Switzerland. This article is an open access article distributed under the terms and conditions of the Creative Commons Attribution (CC BY) license (<http://creativecommons.org/licenses/by/4.0/>).

1. Introduction

The aim of this paper is to present some new geological, seismo-stratigraphic and sedimentological data on the depositional environments recognized in the coastal area surrounding the Cilento Promontory, located in the Southern Tyrrhenian Sea, as derived by the marine geological mapping of the geological sheet n. 502 “Agropoli” [1–3]. The geological sheet n. 502 “Agropoli” (1:50.000 scale) has shown the distribution of several lithostratigraphic units, cropping out at the sea bottom and of the main morphological lineaments, accordingly to the CARG (CARta Geologica) set of rules [4,5]. The main stratigraphic units individuated through the analysis of the sediments cropping out at the sea bottom belong to the Late Quaternary depositional sequence (Figure 1). The spatial and temporal evolution and the lateral and vertical migration of the depositional environments belonging to the Late Quaternary depositional sequence, i.e., the coastal setting, the continental shelf setting and the slope setting, have been previously discussed [6–10]. The variations of the accommodation space of the Late Quaternary deposits during the last fourth-order glacio-eustatic cycle, ranging in age between 128 ky B.P. (Tyrrhenian stage) and the isotopic stage 5 have been recorded by the stratigraphic succession investigated through the marine geological survey. Catuneanu et al. [9] studied the

sequence stratigraphic concepts in detail, particularly referring to the depositional sequences, bounded by subaerial unconformities and their marine correlative conformities. These unconformities have been used as sequence boundaries, marking hiatuses in the stratigraphic record. All the genetic models of the depositional sequences are based on the distinction of forced regressive deposits, normal regressive (lowstand and highstand) deposits and transgressive deposits as distinct genetic units [9]. Forced regressive deposits, normal regressive (lowstand and highstand) deposits and transgressive deposits can be identified when they can be genetically related to the changes in shoreline trajectory [8]. Catuneanu [10] further specified the definition of sequence as a rock-stratigraphic unit bounded by interregional unconformities in the 1940s with a resolution of 10^2 - 10^3 m [11–16], as a relatively conformable succession of genetically related strata bounded by unconformities or their correlative conformities in the 1970s with a resolution of 10^1 - 10^2 m and, finally, as a stratigraphic cycle defined by the recurrence of the same type of sequence stratigraphic surface in the rock record in the 2010 s with a resolution of 1–10 m.

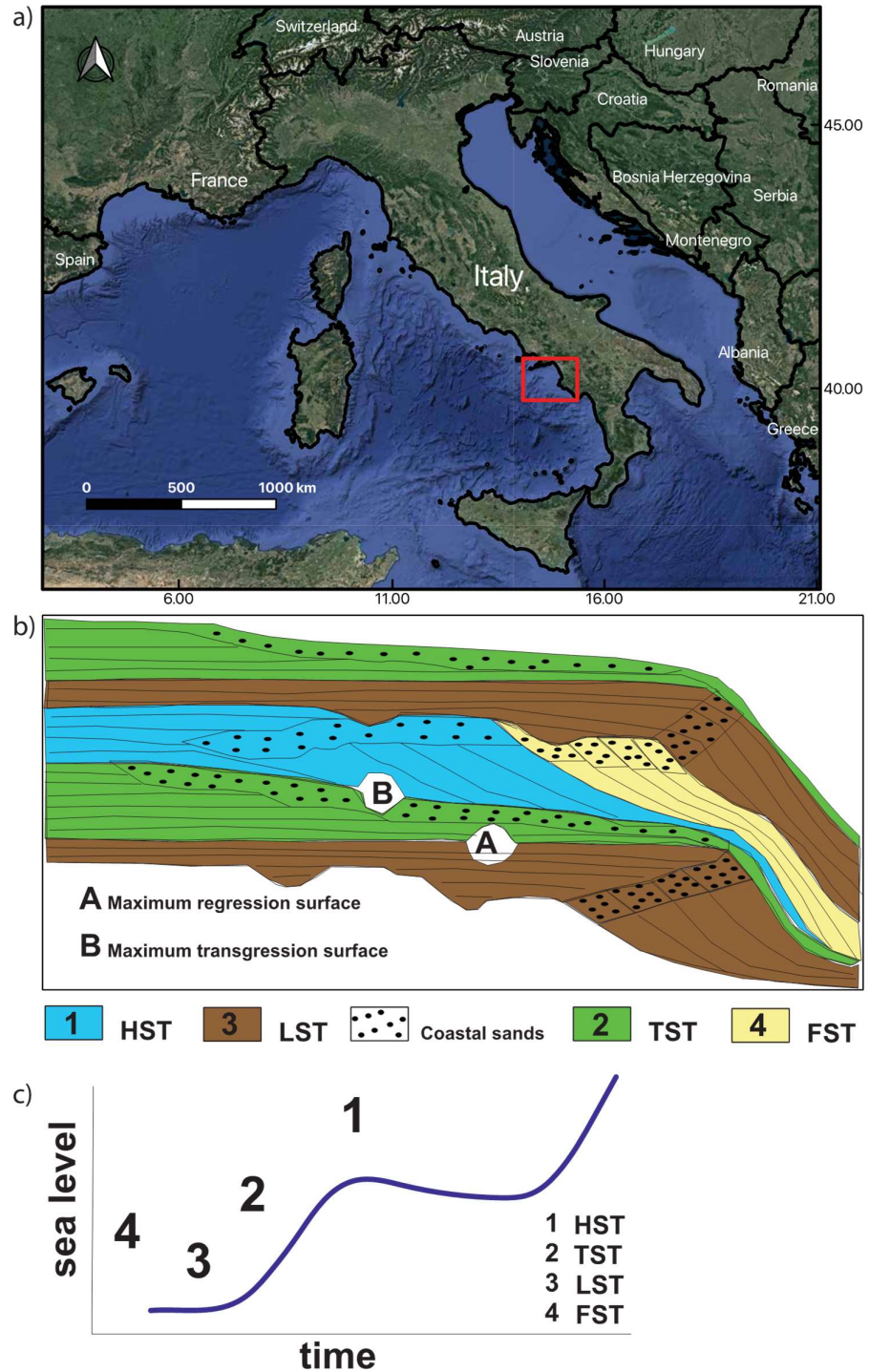


Figure 1. (a) Location map of the study area (red inset). (b) Sketch stratigraphic diagram as a function of depth (c) and time, showing the geometric relationships between the system tracts and the distribution of siliciclastic facies in unconformity-bounded depositional sequences. HST: Highstand system tract. TST: Transgressive system tract. LST: Lowstand system tract. FST: Forced regression system tract.

The facies analysis criteria and the schematic representation of the depositional environments are herein briefly resumed. The system tracts of the Late Quaternary depositional sequence consist of deposits typified by facies genetically related to continental, coastal, shelf and deep-sea depositional environments. Here, we will concentrate on the coastal and continental shelf depositional environments, since the other kinds of deposits have not been recognized in the study area. The coastal depositional systems are characterized by a great variability, both in the morphology and in the depositional style. This variability has suggested different budgets between the available sediments, coupled with the genetic control of the oceanographic regimes (“wave-dominated”, “tide-dominated” or “mixed”) [17–22]. The Mediterranean Sea is typified by a micro-tidal regime. In particular, on the Italian continental margins, the coastal systems are wave-dominated. The coastal deposits grow during each phase of a relative sea level cycle, but with different facies. Regressive systems arise during the sea-level falls (“forced regressions”) [23,24] or when the siliciclastic supply counterbalances the relative sea-level rate. If we consider the present day continental shelf deposits, three main types have been summarized, including the relict sediments, deposited during a seawards advancement of the shoreline and then drowned, the palimpsest sediments, which are relict sediments reworked by currents, storm waves and tides and the Late Quaternary highstand deposits, in equilibrium with the present day depositional processes [25–27]. The highstand deposits are younger than the maximum marine flooding occurred at the end of the last sea-level rise (about 4 to 5 ky B.P.). Offshore Italy, they exhibit their maximum thickness on the inner shelf in correspondence to the main deltas (Po, Tiber and Arno), reduced to a few meters on the outer shelf (Figure 2). In Naples Bay, the highstand deposits have been mapped offshore Campania [28–31].



Figure 2. Satellite map of Italy, showing the main river systems (Po, Tiber and Arno) whose deltas have fed the highstand deposits of the Italian continental shelf.

Maërl layers (Maërl is a hard seaweed with a purple-pink color that forms reef-like carpets, known as maërl beds, in the dim light conditions of the shallow seas along the European coasts) have been recognized on the continental shelf offshore Cilento through the geological interpretation of sub-bottom profiles [32]. The maërl facies has been recognized based on the component analysis of 32 grab samples and is preferentially concentrated on the submerged depositional terraces, located at water depths ranging be-

tween 42 m and 52 m. This preferential distribution has been probably controlled by strong bottom currents occurred in this area due to the local oceanographic circulation, preventing for the deposition of siliciclastic deposits. The coralline algae have controlled the carbonate deposition offshore the Cilento Promontory at water depths ranging between 40 m and 60 m [32]. Another significant contribution to the depositional environments deals with the searching of relict sandy deposits on the continental shelf offshore the Cilento Promontory aimed at beach nourishment [33]. The performed analyses have allowed to individuate the submarine relict sands suitable for beach nourishment. Moreover, the terraced landforms occurring both onshore and offshore the Cilento Promontory have been recently analyzed and aimed at reconstructing the meaning of the terraced surfaces as Quaternary records of the sea level changes [34]. Two main types of terraced surfaces have been recognized, including the erosional terraces (“wave-cut platforms” or “abrasion platforms”) [35–37] and the depositional terraces (STDs) [38–40]. Two types of landforms have been controlled by the interaction of several geological processes, including the type of bedrock, the geodynamic setting, the sedimentary input and the relative sea level changes [34]. In the Cilento offshore, the submarine marine terraces were formed when the rocky outcrops were exposed on the continental shelf and were predominantly generated during the interglacial periods [34].

In this paper, the marine geological maps have allowed to show the depositional environments occurring offshore of the Cilento Promontory and to interpret these environments in terms of system tracts of the Late Quaternary depositional sequence [41–43]. Moreover, the sedimentological data of sea bottom samples have been analyzed in order to show the main grain sizes occurring at the sea bottom in this portion of the Cilento offshore. Ternary plots have been constructed in order to evaluate the different grain sizes, considering as variables shale, sand and silt and gravel and sand and silt, respectively. These plots allowed to analyze the grain sizes occurring at the sea bottom in this portion of the Cilento offshore. Sub-bottom profiles have been interpreted based on the criteria of seismic stratigraphy in order to reconstruct the stratigraphic setting of the area and to complement the cartographic representation.

2. Geologic Setting

The Southeastern Tyrrhenian margin is a passive-type continental margin involved by listric faults, with blocks dipping both seawards and landwards. Along the Tyrrhenian margin, this tectonic style has controlled the formation of half-graben basins on the continental shelf and slope, alternating with structural highs [44,45].

The marine area surrounding the Cilento Promontory represents a structural high resulting from the seawards prolongation of the Licosa Cape structural high, bounded northwards and southwards by two half-graben basins: the Salerno Valley and the Policastro Gulf. The Salerno Valley is a half-graben basin whose individuation has been controlled during the Early Pleistocene by the master fault Capri-Sorrento Peninsula, with average throws in the order of 1500 meters [46,47]. Previous seismo-stratigraphic data have shown a main regional unconformity, located at depths ranging between 2000 and 2500 meters, correlated with the top of the Meso-Cenozoic carbonates and marking the base of the Plio-Pleistocene filling of the Salerno Valley [46,47].

The Cilento structural high has been deeply investigated based on its geologic and seismo-stratigraphic characteristics. The interpretation of multichannel profiles has shown the occurrence of wide structural highs, characterized by an acoustically transparent seismic facies, corresponding to the acoustic basement, alternating with parallel seismic reflectors corresponding to the Quaternary marine filling of sedimentary basins [48]. More recently, the geological interpretation of newly acquired deep multichannel seismic lines along the Tyrrhenian margin has confirmed this structural framework, showing that the geological structure of the Cilento high is locally complicated by folding, reverse faults and basin inversions [49–51].

In the Cilento Promontory, the siliciclastic successions of the Cilento Flysch crop out, which have involved the deformation of the Apenninic chain during the Cenozoic and have been then deformed by the Plio-Quaternary extensional tectonic phases [52–54]. These units have been deeply revised from a stratigraphic and structural point of view [53]. The revision was focused both on the Cilento Group, composed of the “Pollica” Sandstones and of the “S. Mauro” Formation and on the Northern Calabria Unit, constituted by the “Crete Nere” Formation, by the “Saraceno” Formation, by the “Cannicchio” Sandstones and by the “Sicilide” units [53]. These stratigraphic-structural units represent the rocky acoustic basement of the Plio-Pleistocene and Holocene marine deposits of the continental shelf between the Licosa Cape and the Palinuro Cape—namely, the ssi unit described in this paper (see the section on the results).

3. Materials and Methods

The research has been developed through the acquisition, the processing and the geologic interpretation of a densely spaced grid of high-resolution seismic profiles (sub-bottom Chirp) collected by the CNR-ISMAR onboard of the R/V Urania (National Research Council of Italy). The grid of sub-bottom Chirp profiles superimposed to the onshore–offshore DEM of the Cilento Promontory is reported in Figure 3. The acoustic profiling system CAP-6600 Chirp II has been used. Its linear frequency modulated signals of 2–7 kHz or 8–23 kHz and 4-kW provide high-resolution sounding reaching a 10–30-cm resolution within uppermost marine sediments. The obtained data, recorded onboard with a SEG-Y format, was processed by using the software Seisprho [55], allowing to plot the sub-bottom profiles as bitmap images. The geological interpretation of sub-bottom profiles was carried out based on the criteria of seismic stratigraphy in order to identify the main seismic sequences and the related unconformities [56].

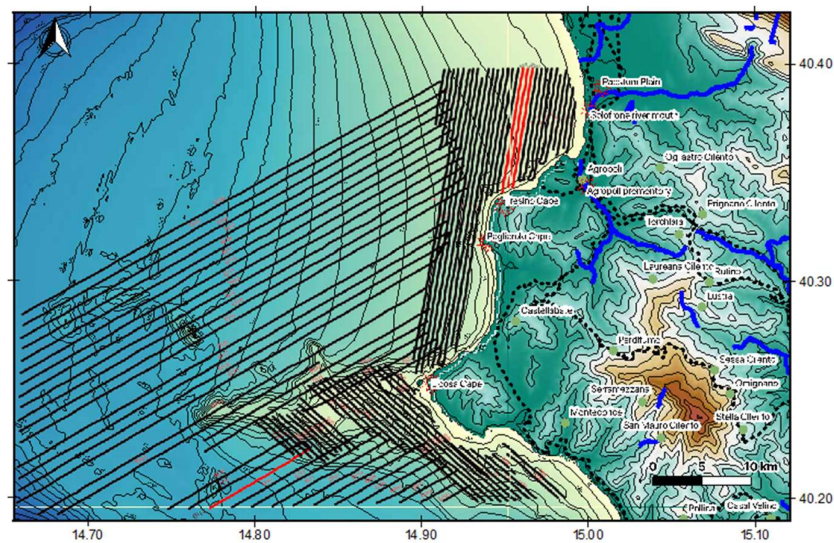


Figure 3. Location map of sub-bottom Chirp profiles superimposed to onshore–offshore DEM of the Cilento Promontory. Red lines indicate the seismic profiles shown in the text.

The sea bottom samples were collected during the GMS 03_01 cruise (R/V Urania, CNR) in November 2003 by a Van Veen grab and immediately described in terms of visible features and grain size. The location of samples superimposed on the onshore–offshore Digital Elevation Model (DEM) of the Cilento offshore is shown in Figure 4. The grain size analyses were performed at the CNR-ISMAR (Naples, Italy) sedimentological laboratory using a grain size laser analyzer (SYMPATEC Laser Particle Size Analyzer).

The particle size analysis involved a phase of preparation and pre-treatment of the sample. The collected samples were dried in thermostatic ovens at 105 °C for 24 hours, until the weight stabilization was obtained. Then, the pretreatment was carried out with a solution of hydrogen peroxide and distilled water for 24/48 hours. Subsequently, the sample was stirred with a mechanical stirrer at 600 rpm for about 2 hours and then wet-separated with a 63- μm sieve into a coarse component ($> 63 \mu\text{m}$) and a fine component ($< 63 \mu\text{m}$). The coarse fraction was dry screened with a stack of ASTM sieves with mesh sizes ranging from 4000 μm to 63 μm , with intermediate sieves and a subsequent determination of the weights of the obtained fractions. The fine fraction was first analyzed dry, until a sub-sample was obtained, dispersed in an aqueous solution and subsequently analyzed with the laser granulometer. The processed sedimentological data were used for the construction of cumulative and frequency curves and were classified according to the classification of Shepard (1954), classical or modified.

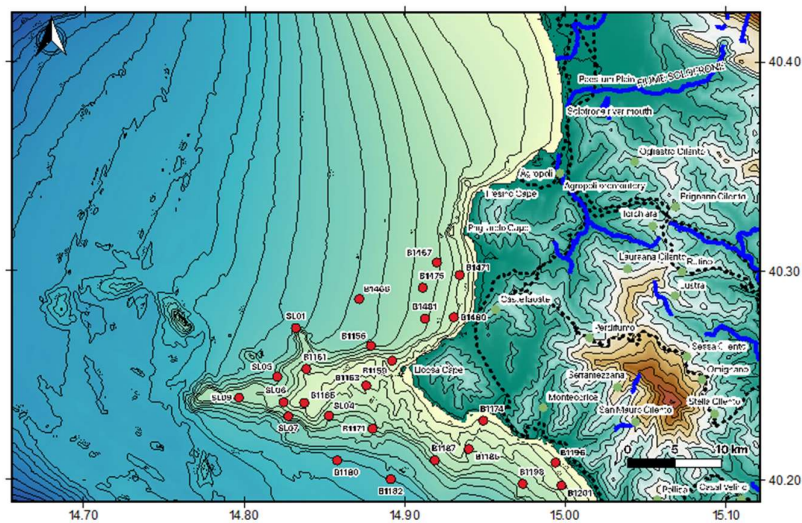


Figure 4. Location of sea bottom samples superimposed on onshore–offshore DEM of the Cilento offshore.

4. Results

Marine geological mapping (Figure 5) coupled with sedimentological and seismic-stratigraphic data has allowed to reconstruct the depositional environments offshore of Northern Cilento. Four geological maps show the distribution of the Late Quaternary deposits at the seafloor in the Cilento offshore and have been superimposed to the onshore–offshore DEM of the Cilento Promontory (Figure 5).

The map n. I NW (scale 1: 25.000) covers a continental shelf area, dipping with low gradients up to water depths of 95 m (Figure 5). The northeastern extremity of this map, including the farthest southern sector of the Paestum Plain, includes little ramps up to water depths of 35 m. The rocky shoreline and the outcrops of acoustic basement alongside the Agropoli promontory control the convex bathymetric trend up to 25 m. Similarly, the rocky promontory between the Tresino Cape and the Pagliarolo Cape conditioned the physiography of the submerged area, with a convex bathymetric trend surrounding high coastlines. The physiographic unit of the Licosa Cape high, represented by an E–W trending ridge, is the most representative morpho-structural lineament of both maps n. II SW and n. III SE (scale 1: 25.000; Figure 5). An articulated E–W bathymetric trend occurs, with a wide area showing remnants of terraced surfaces located at different water depths [3,34]. The concave bathymetric trend highlights the occurrence of slide scars, incised by drainage axes, in the southern sector of the structural high. Three main morpho-structural highs of the acoustic basement occur, respectively, N–S, E–W and

NNW–SSE trending (Figure 5). A continental shelf, ranging at water depths between 105 and 185 m, is covered by the map n. IV NE (scale 1: 25.000; Figure 5).

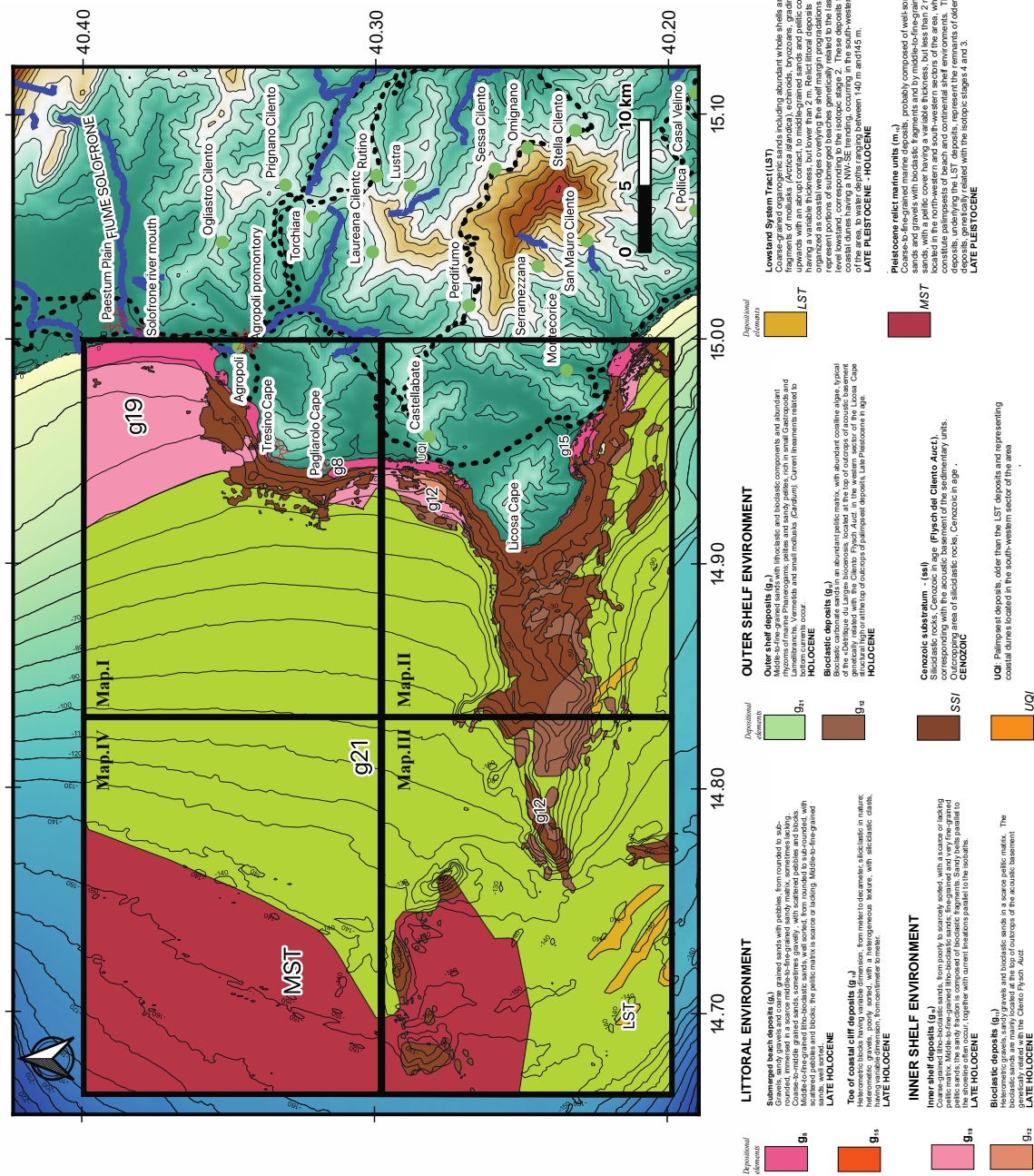


Figure 5. Onshore-offshore DEM of the Cilento Promontory with superimposed the results of the marine geological survey at the 1:25.000 scale (map n. I NW, map n. II SW, map n. III SE and map n. IV NE).

The submerged beach deposits and the toe-of-coastal cliff deposits, particularly abundant at the foot of the present day coastal cliffs, incised in Pollica formation, characterizing the littoral environment. Next to Licosa Cape, the toe-of-coastal cliff deposits surrounded a wide terrace of marine abrasion, located at water depths ranging between 4 m and 10 m, extending from the S. Marco Plain to Ogliastro Marina Bay. Poorly sorted blocks and gravels constitute the toe-of-coastal cliff deposits. The submerged beach deposits are composed of gravels, sandy gravels and coarse-grained sands with rounded to

subrounded pebbles, immersed in a scarce middle-to-fine-grained sandy matrix. The inner shelf deposits and the bioclastic deposits characterize the inner shelf environment. The inner shelf deposits are composed of poorly sorted coarse-grained litho-bioclastic sands, middle-to-fine-grained litho-bioclastic sands and fine-grained pelitic sands. The bioclastic deposits are composed of bioclastic gravels, gravelly sands and bioclastic sands immersed in a scarce pelitic matrix. The bioclastic sands often represent the base of meadows of marine Phanerogams and are located at the top of wide outcrops of the Cenozoic substratum (ssi unit), genetically related with the Cilento Flysch, based on criteria of stratigraphic correlation of the geological units cropping out in the adjacent emerged coastal belt with the corresponding geological units recognized offshore. The outer shelf deposits and the bioclastic deposits characterize the outer shelf environment. The outer shelf deposits are composed of middle-to-fine-grained sands with lithoclastic and bioclastic fragments, including abundant rhizomes of marine Phanerogams, and of pelites and sandy pelites. Bioclastic sands in a pelitic matrix, with abundant calcareous algae, constitute the bioclastic deposits.

The sedimentological analyses disclose the grain size distribution of the sediments at the seafloor offshore the Cilento Promontory. The recognized grain sizes include sandy gravels, gravelly sands, sands, silty sands, muddy sands, sandy silts, silts and muds. The results of the sedimentological investigation showed that the analyzed samples mainly consist of fine-grained lithologies. Fine-grained sands are widespread along the coast in the northern sector of the study area. Offshore of Licosa Cape, both fine-grained and coarse-grained sands were recognized. Ternary plots of sea bottom samples (Figure 6) were constructed (shales–sands–silts) and (gravels–sands–silts) in order to improve the processing of the sedimentological data and to elaborate the sedimentological results.

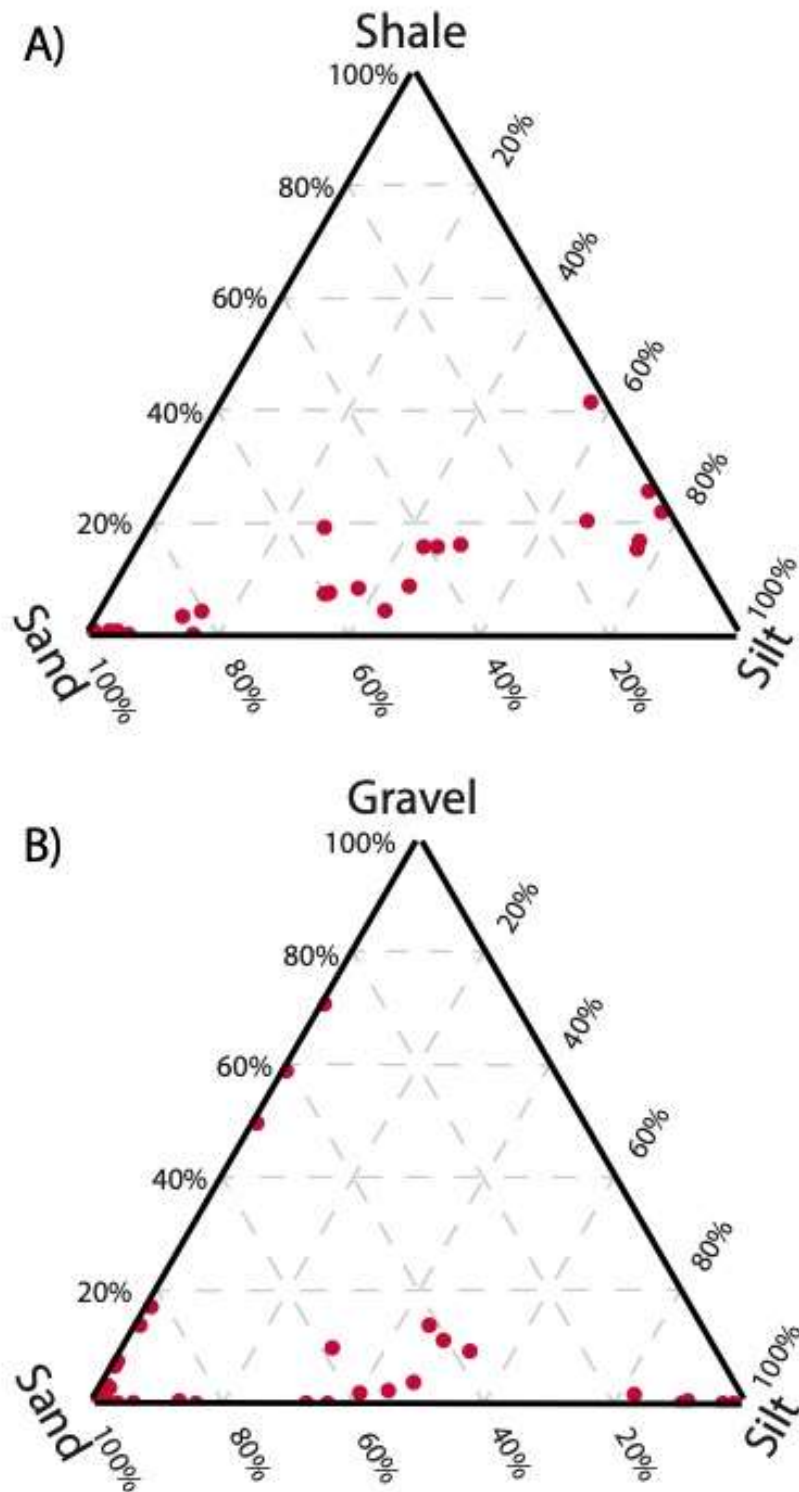


Figure 6. Ternary plots of the sea bottom samples. Inset (A): ternary plot shale-sand-silt. Inset (B): ternary plot gravel-sand-silt.

The seismic analysis of the sub-bottom Chirp profiles has allowed us to study the seismo-stratigraphic characteristics of the Cilento offshore between the Solofrone river mouth and the Licosa Cape. The main outcrops at the sea bottom of the rocky acoustic basement were bounded, relatively to the sedimentary covers, composed of

coarse-grained sands grading towards middle-fine-grained sands and fine-grained sands. The sandy facies are prevalent in the sector of continental shelf located between the Solofrone river mouth and Agropoli Town, where they form N–S sandy belts parallel to the isobaths and located at water depths ranging between 10 and 17 m. In the same area, the rocky outcrops have a limited extension and occur at water depths ranging between 15 m and 20 m.

The rocky acoustic basement (ssi) widely crops out next to the shoreline from Agropoli Town to Tresino Cape and from Tresino Cape to Pagliarolo Cape, where it represents the seawards prolongation of the coastal cliffs incised in the deposits of the Cilento Group [52–54]. From Agropoli to Tresino Cape, the ssi unit is represented by a terraced surface having a low gradient, dipping seawards and outcropping at the sea bottom at water depths ranging between 5 m and 25 m. In this area, the basement is colonized by *Posidonia* meadows. From Tresino Cape and Pagliarolo Cape, the rocky substratum forms a terraced surface having a low gradient between the emerged sea cliff and the isobath of 20 m, physically continuous, lacking the adjoining sandy facies of a submerged beach. This outcrop strongly reshapes the trending of the two rocky promontories on-shore, showing the strong control played by the land geology on the marine geology. In the whole sector, the acoustic basement is downthrown below the recent sedimentary cover through normal faults, whose upper part is sometimes evident on seismic profiles.

The seismo-stratigraphic analysis evidenced that the recent sedimentary cover, ranging in age between the Late Pleistocene and the Holocene, is organized into four main seismo-stratigraphic units (Figure 7), overlying the undifferentiated acoustic basement (ssi). The first unit (seismo-stratigraphic unit 1) is characterized by an acoustically transparent seismic facies and ranges in thickness between 7 m and 10 m. Unit 1, probably composed of sands, unconformably overlies the undifferentiated acoustic basement (ssi). Its top is strongly eroded, forming palaeo-channels, in which the seismo-stratigraphic unit 2 was deposited.

The second unit (seismo-stratigraphic unit 2; Figure 7) is distinguished from alternating acoustically transparent intervals and continuous intervals, probably corresponding with alternating sands and shales for a whole thickness of about 10 meters. The unit forms the filling of depressions or intra-platform basins individuated at the top of unit 1 and of erosional depressions located at the top of the unit ssi.

The third unit (seismo-stratigraphic unit 3; Figure 7) is characterized by acoustic facies with parallel and discontinuous reflectors of high amplitude and represents a first phase of the recent filling, Holocene in age.

The fourth unit (seismo-stratigraphic unit 4; Figure 7) is distinguished from seismic facies with parallel continuous-to-discontinuous reflectors of high amplitude and represents a second phase of the recent filling, Holocene in age. The geological interpretation of sub-bottom profiles has shown the occurrence of shallow gas pockets (Figure 7).

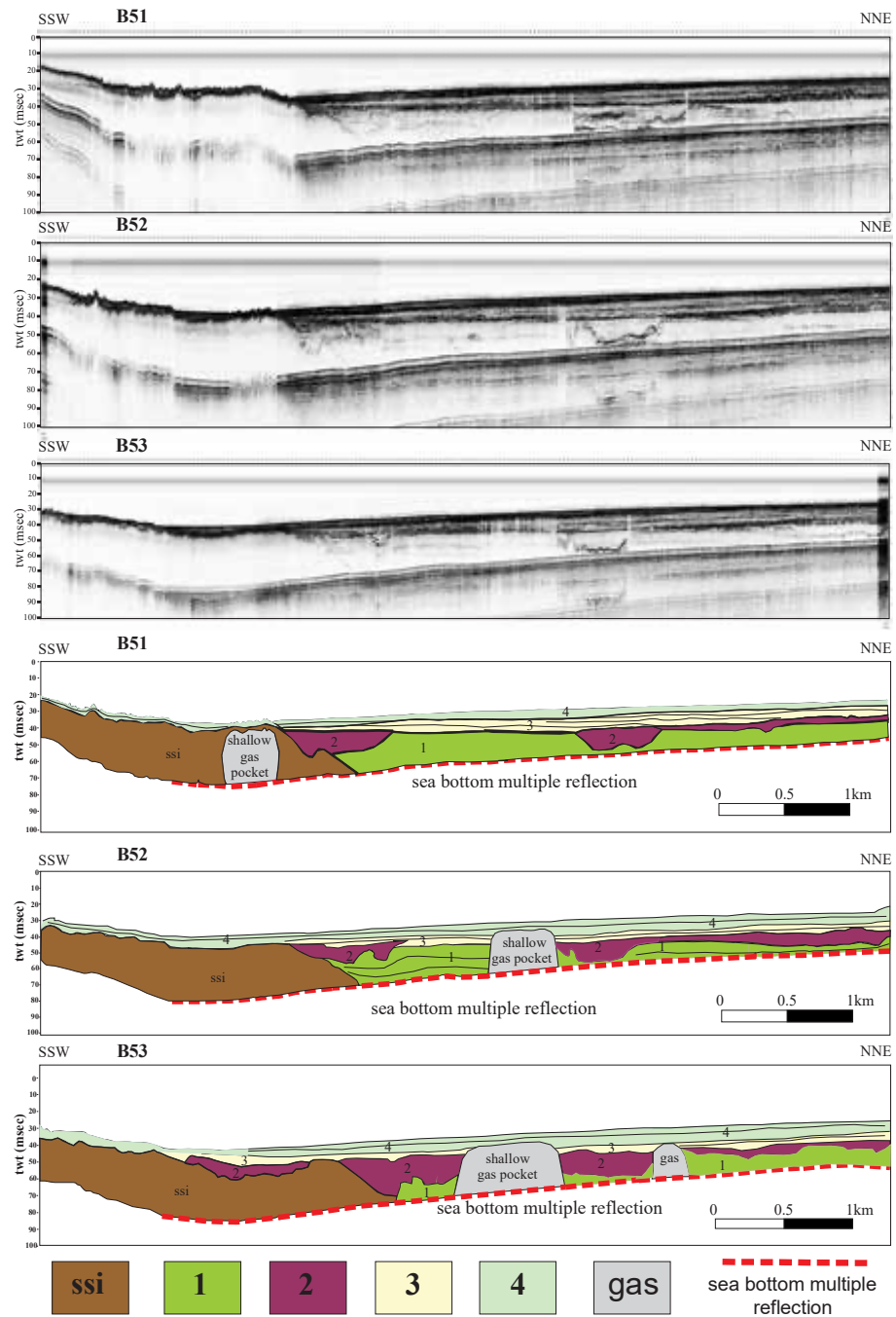


Figure 7. Sub-bottom profiles B51, B52 and B53 and the corresponding geological interpretations (see Figure 3 for location).

The seismo-stratigraphic interpretation of the sub-bottom profile B114 was calibrated with the lithostratigraphic data of a gravity core, herein named the Licosa gravity core, previously published (Figure 8) [57]. On the left in the seismic profile, the rocky acoustic basement genetically related with the Cilento Flysch (ssi unit) was recognized. This seismic unit is overlain by a thick progradational unit, interpreted as the beach deposits of the isotopic stages 4 and 5 [58,59], Late Pleistocene in age. Based on the calibration with the Licosa gravity core, the uppermost part of this unit has been interpreted as coarse-grained sands, very rich in Mollusk shells, including *Arctica islandica*, a cold host

of the Pleistocene (Sg unit; Figure 8). This represents a key seismic unit in the seismic-stratigraphic setting of this area and is composed of coarse-grained organogenic sands. Being located at higher water depths with respect to the sedimentary distribution model, which locates this kind of organogenic sand in the coastal belt [60,61], this unit can be interpreted as relict sands [62], which can be compared with the organogenic sands described by Péres and Picard (1964) [63], including cold hosts attributed to the end of the Würm.

The Sg unit forms a sandy ridge, which is located at water depths ranging between 130 m and 140 m of the water depth (Figure 8). This sandy ridge has been interpreted as a part of the submerged beach (shoreface) and could be related to the last lowstand phase, corresponding to the isotopic stage 2 [58,59]. The underlying seismic unit, characterized by pro-grading clinoforms, could represent the remnants of older beach systems, genetically related with the isotopic stages 4 and 3 (Late Pleistocene; Figure 8).

The abrupt contact between the coarse-grained sands with *Arctica islandica* and the overlying finer-grained deposits (Sm to Ag deposits in the Licosa core; Figure 8) is represented by an erosional surface (“ravinement surface”; Figure 8) [64]. The ravinement surface is a time-transgressive or diachronous subaqueous erosional surface resulting from nearshore marine and shoreline erosion associated with a sea level rise [64]. Proceeding landwards, this erosional surface laterally grades into the erosional surface located at the top of the rocky acoustic basement (Figure 8).

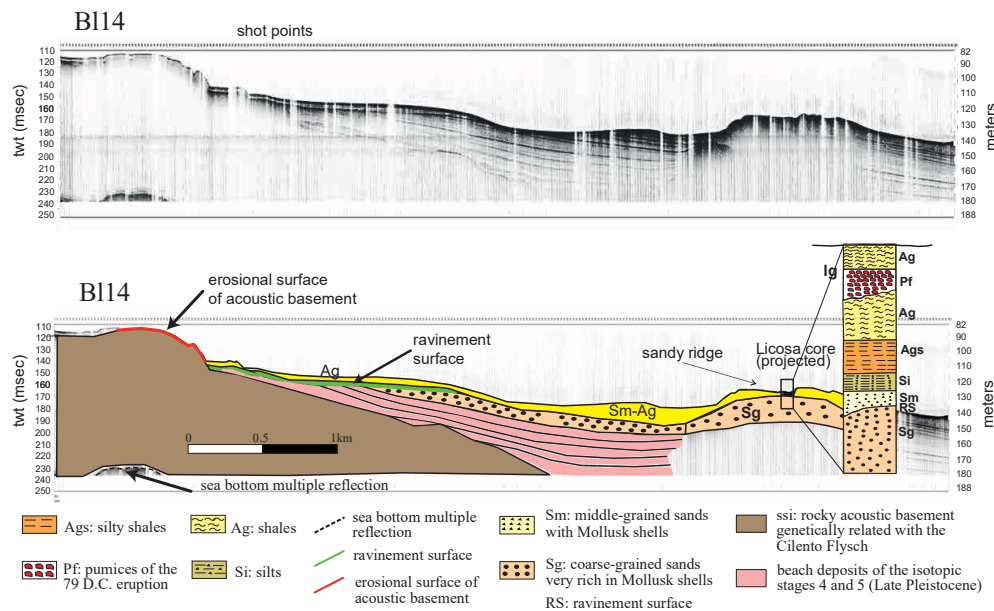


Figure 8. Sub-bottom profile B114 and corresponding geologic interpretation, calibrated with the lithostratigraphic data of the Licosa gravity core (see Figure 3 for location). The subfigure on the right side of the seismic profile represents the stratigraphy of the Licosa core (see the key to the seismic profile for the explanation).

5. Discussion

The seismic and sequence stratigraphy are techniques of the analysis of seismic profiles that have undergone a rapid evolution, starting from the basic concepts of Vail et al. 1977 [6]. In this paper, a definition of the depositional sequence was given, coupled with the criteria for its determination, based on the lateral terminations of the inner strata of sequences, both upwards (erosional truncation) and downwards (onlap and downlap). These criteria were and still remain basic for the identification of regional unconformities bounding the depositional sequences in their lower part and in their upper part. Other basic concepts of this technique have been developed by Christie-Blick 1991 [7], who de-

fined, for the first time, the “unconformity-bounded” depositional sequences based on their stratal patterns (onlap and offlap). In particular, the “unconformity-bounded” depositional sequences show onlapping strata at their base and offlapping strata at their top [7]. Despite how many sequence stratigraphic papers have been further developed, reaching the modern applications and concepts of sequence stratigraphy of Catuneanu [9,10], we believe that some basic concepts of the first sequence stratigraphic papers are still valid [6–8], as the identification of regional unconformities for the identification of the depositional sequences.

Based on marine geological mapping, coupled with seismo-stratigraphic interpretation and confirmed by the sedimentological data, all the described deposits (littoral, inner shelf and outer shelf environments) pertain to the highstand system tract of the Late Quaternary depositional sequence (Figure 5). The lowstand system tract is composed of organogenic coarse-grained sands, including an abundant bioclastic component (Mollusks, Echinoids, Bryozoans), passing upwards through an abrupt contact to middle-grained sands and thin pelitic drapes, whose thickness does not exceed 2 m (Figure 5). They are relict littoral deposits, organized as coastal wedges overlying the shelf margin prograding clinoforms, which represent portions of submerged beaches genetically related with the last sea-level lowstand, corresponding with the isotopic stage 2 [58,59]. The lowstand deposits form dune strips with NW-SE elongation, which occur in the southwestern sector of the area, at water depths ranging between 140 m and 145 m (Figure 5). The Pleistocene relict marine units are composed of coarse-to-fine-grained marine deposits and are probably constituted by well-sorted sands and gravels with bioclastic fragments and by middle-to-fine-grained sands overlain by thin pelitic drapes not exceeding a thickness of 2 m. These deposits, which constitute palimpsests of beach and continental shelf environments, are mainly located in the northwestern and southwestern quadrants of the marine area covered by the geological sheet n. 502 “Agropoli”. These deposits, underlying the lowstand system tract represent the remaining parts of older beach systems correlated to isotopic stages 4 and 5 [58,59] (Figure 8).

The bioclastic deposits are typical of the biocenosis of “Détritique Du Large” [63], developed on hard sea bottoms and are located both at the top of outcrops of Cenozoic acoustic basement, genetically related with the Cilento Flysch (ssi unit) in the western sector of the morpho-structural high of the Licosa Cape and at the top of palimpsest deposits, Late Pleistocene in age (Figure 5). In the Mediterranean Sea, the zonation of benthic assemblages carried out by Péres and Picard [63] represents a basic tool in order to know the lithology and to interpret the facies of the bioclastic deposits (Figure 9). In the Mediterranean Sea, the bioclastic deposits occur at water depths ranging between 40 m and 100 m (“Détritique Cotier” of Péres and Picard) [63] (Figure 9). The main components of this biocenosis are produced after the reworking and the deposition of the benthic communities on both mobile sea bottoms (biocenosis of the “Détritique Cotier”) and on hard sea bottoms (biocenosis of the “Détritique Du Large”). After the Holocene, sea level rise relict and drowned sediments, characterized by low rates of sedimentation and by the occurrence of glauconite, were deposited on the seafloor (“Détritique Du Large”; Figure 9) [64,65].

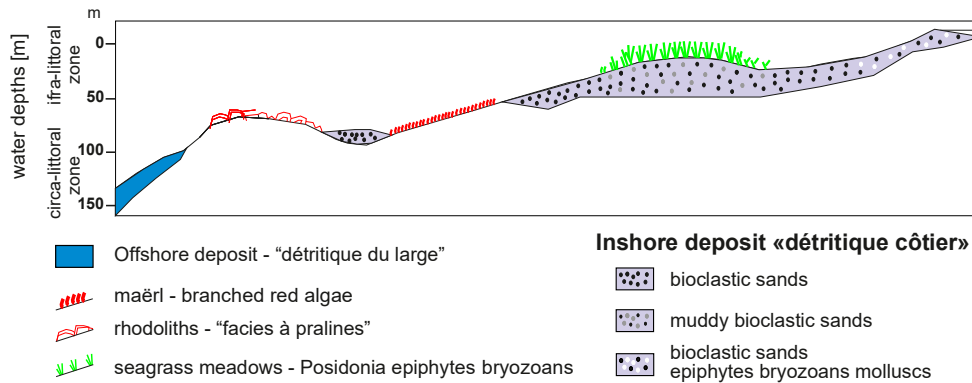


Figure 9. Sketch diagram showing the main biocenosis of the mobile sea bottoms.

6. Conclusions

The geological evolution of the Cilento continental shelf during the Late Pleistocene-Holocene has been reconstructed based on the marine geological data (Figure 5), coupled with the sedimentological data (Figure 6) and with the seismo-stratigraphic data (Figures 7 and 8).

Following a general climate warming [66–69], during the Upper Pleistocene Holocene, there was a rapid rise of sea level on a global scale [70–74]. Transgressive and highstand deposits have been individuated on the continental shelves all around the world [26,75–80]. During the transgression, the high rate of the sea level rise and the low gradient of the Cilento continental shelf led to the almost simultaneous submersion of large areas and to the drastic landwards shift of the coastal facies. As a consequence, the geological interpretation of the Chirp sub-bottom profiles did not allow the identification of retrogradational seismo-stratigraphic units, which can be interpreted as beach systems deposited during the transgression. On the contrary, highstand and lowstand deposits have been well-documented based on seismo-stratigraphic data (Figures 7 and 8).

The ravinement surface, representing an erosional truncation involving the upper part of the offlap succession, is characterized by an irregular topography (Figure 8). The Licosa core, calibrating the sub-bottom profile B114 (Figure 8), has shown that the sediments overlying the ravinement surface are characterized by middle-grained sands grading upwards into silty shales (Sm, Si, Ags; Figure 8), with an overall decrease of the grain size upwards. This decrease in grain size indicates a deepening of the continental platform. These sediments have been interpreted as deposited during the transgressive phase started at the end of the glacial stage of the isotopic stage 2 [57]. These deposits are overlain, in turn, by shales (Ag), including a pumiceous ash layer of Vesuvius, and are located on the ravinement surface (Figure 8). In the sub-bottom profile B114, this succession (transgressive and highstand deposits) constitutes a thin drape overlying the ravinement surface (Figure 8). Unfortunately, tephrostratigraphic data on this layer are not still available, allowing it to function as a good chronostratigraphic layer in this sector of the Tyrrhenian margin.

From the end of the isotopic stage 5a, the sea, despite the cyclical oscillations, is constantly lowering up to the isotopic stage 2, when it was located at a depth of about 120 m in the Mediterranean Sea [16,81–90]. During this phase of “forced regression” [24,91–94], the progradational wedges of the Cilento offshore were deposited, allowing for a platform widening in the order of several kilometers. The forced regression is controlled by the seaward migration of the coastline as a reaction to the relative sea-level fall. This kind of regression occurs during periods of falling of the sea level, since the coastline is forced to regress due to the falling of the base level, without taking into account the sediment supply [24]. During the forced regression, the fluvial incision is accompanied by the deposition of pro-gradational deposits, in a shoreface setting.

Author Contributions: Writing, original draft preparation; data interpretation and writing, review and editing, G.A.; Methodology, software and data curation, M.C. All authors have read and agreed to the published version of the manuscript.

Funding: This research received no external funding, but the analyzed data were acquired by the CNR ISMAR of Naples (Italy) in the frame of the realization of the geological sheet n. 502 “Agropoli” (marine sector). The CARG Project was previously funded by the National Research Council of Italy (CNR-IAMC, now CNR-ISMAR) and by the Campania Region-Sector of Defence Soil, Geothermics and Geotechnics, Naples Italy.

Institutional Review Board Statement: Not applicable.

Informed Consent Statement: Not applicable.

Acknowledgments: We thank the Academic Editor Antoni Calafat and two anonymous reviewers, whose comments greatly improved this manuscript. We thank Lucia Monti for making available the data shown in this paper.

Conflicts of Interest: The authors declare no conflicts of interest.

References

1. Aiello, G.; Marsella, E. The contribution of marine geology to the knowledge of marine coastal environment off the Campania region (southern Italy): The geological map n. 502 “Agropoli” (southern Campania). *Mar. Geophys. Res.* **2013**, *34*, 89–113. <https://doi.org/10.1007/s11001-013-9186-4>.
2. Martelli, L.; Nardi, G.; Cammarosano, A.; Cavuoto, G.; Aiello, G.; D’Argenio, B.; Marsella, E.; Ferraro, L. *Note Illustrative Della Carta Geologica d’Italia Alla Scala 1:50.000*; Regione Campania, ISPRA (Servizio Geologico d’Italia), Rome, Italy: **2016**; pp. 1–110. Available online: http://www.isprambiente.gov.it/Media/carg/note_illustrative/502_Agropoli.pdf. Accessed online on 4th October 2021.
3. Aiello, G. Elaborazione ed interpretazione geologica di sismica di altissima risoluzione nell’offshore del promontorio del Cilento (Tirreno meridionale, Italia). *Quad. Geofis.* **2019**, *155*, 1–24. <https://doi.org/10.13127/qdg/155>.
4. Catalano, R.; Fabbri, A.; Argnani, A.; Bortoluzzi, G.; Correggiari, A.; Gamberi, F.; Ligi, M.; Marani, M.; Penitenti, D.; Roveri, M.; et al. *Linee Guida al Rilevamento Delle Aree Marine del Servizio Geologico Nazionale*; Bozza n. 1; APAT, Servizio Geologico d’Italia: Rome, Italy, 1996.
5. Fabbri, A.; Argnani, A.; Bortoluzzi, G.; Correggiari, A.; Gamberi, F.; Ligi, M.; Marani, M.; Penitenti, D.; Roveri, M.; Trincardi, F. *Carta Geologica Dei Mari Italiani Alla Scala 1:250,000. Guida Al Rilevamento*; Quaderni serie III; Presidenza del Consiglio dei Ministri, Dipartimento per i Servizi Tecnici Nazionali, Servizio Geologico d’Italia, Rome, Italy: **2002**; Volume 8, pp. 1–93.
6. Vail, P.R.; Mitchum, R.M.; Todd, R.G.; Widmier, J.M.; Thomson, S.; Sangree, J.B.; Bubb, J.N.; Hatlelid, W.J. Seismic stratigraphy and global changes of sea level. In *Seismic Stratigraphy—Applications to Hydrocarbon Exploration*; Payton, C.E., Ed.; Mem. 26; American Association of Petroleum Geologists: Tulsa, OK, USA, **1977**; pp. 49–212.
7. Christie-Blick, N. Onlap, offlap, and the origin of unconformity-bounded depositional sequences. *Mar. Geol.* **1991**, *97*, 35–56. [https://doi.org/10.1016/0025-3227\(91\)90018-Y](https://doi.org/10.1016/0025-3227(91)90018-Y).
8. Helland-Hansen, W.; Gjelberg, G.J. Conceptual basis and variability in sequence stratigraphy: A different perspective. *Sediment. Geol.* **1994**, *92*, 31–52. [https://doi.org/10.1016/0037-0738\(94\)90053-1](https://doi.org/10.1016/0037-0738(94)90053-1).
9. Catuneanu, O.; Abreu, V.; Bhattacharya, J.P.; Blum, M.D.; Dalrymple, R.W.; Eriksson, P.G.; Fielding, C.R.; Fisher, W.L.; Galloway, W.E.; Gibling, M.R.; et al. Towards the standardization of sequence stratigraphy. *Earth-Sci. Rev.* **2009**, *92*, 1–33. <https://doi.org/10.1016/j.earscirev.2008.10.003>.
10. Catuneanu, O. Model-independent sequence stratigraphy. *Earth-Sci. Rev.* **2018**, *188*, 312–388. <https://doi.org/10.1016/j.earscirev.2018.09.017>.
11. Di Capua, A.; Scasso, R.A. Sedimentological and petrographical evolution of a fluvio-lacustrine environment during the onset of volcanism: Volcanically-induced forcing of sedimentation and environmental responses. *Sedimentology* **2020**, *67*, 1879–1913. <https://doi.org/10.1111/sed.12681>.
12. Giannetti, B.; De Casa, G. Stratigraphy, chronology and sedimentology of ignimbrites from the white trachytic tuff, Roccamonfina Volcano, Italy. *J. Volcanol. Geotherm. Res.* **2000**, *96*, 243–295. [https://doi.org/10.1016/S0377-0273\(99\)00144-4](https://doi.org/10.1016/S0377-0273(99)00144-4).
13. Lucchi, F. On the use of unconformities in volcanic stratigraphy and mapping: Insights from the Aeolian Islands (Southern Italy). *J. Volcanol. Geotherm. Res.* **2019**, *385*, 3–26. <https://doi.org/10.1016/j.jvolgeores.2019.01.014>.
14. Available online: <https://stratigraphy.org/guide/uncon>. Accessed online on 4th October 2021.
15. Martinson, D.G.; Pisias, N.J.; Hays, J.D.; Imbrie, J.; Moore, T.C.; Shackleton, N.J. Age dating and the orbital theory of the ice ages: Development of a high-resolution 0 to 300,000-year chronostratigraphy. *Quat. Res.* **1987**, *27*, 1–29. [https://doi.org/10.1016/0033-5894\(87\)90046-9](https://doi.org/10.1016/0033-5894(87)90046-9).
16. Lisiecki, L.E.; Raymo, M.E. A Pliocene-Pleistocene stack of 57 globally distributed benthic $\delta^{18}\text{O}$ records. *Paleoceanography* **2005**, *20*, PA1003. <https://doi.org/10.1029/2004PA001071>.

17. Reading, H. *Sedimentary Environments and Facies*, 1st ed.; Elsevier: New York, NY, USA, 1978; pp. 1–557. <https://doi.org/10.1002/esp.3290060116>.
18. Nummedal, D.; Swift, D.J.P. Transgressive stratigraphy at sequence-bounding unconformities: Some principles derived from Holocene and Cretaceous examples. In *Sea Level Fluctuation and Coastal Evolution*, 1st ed.; Nummedal, D., Pilkey, O.H., Howard, J.D., Eds.; SEPM: Tulsa, OK, USA, 1987; Volume 41, pp. 241–260.
19. Trincardi, F.; Correggiari, A.; Roveri, M. Late Quaternary transgressive erosion and deposition in a modern epicontinental shelf: The Adriatic Semienclosed Basin. *Geo-Mar. Lett.* **1994**, *14*, 41–51.
20. Chiocci, F.L.; Ercilla, G.; Torre, J. Stratal architecture of Western Mediterranean Margins as the result of the stacking of Quaternary lowstand deposits below glacio-eustatic fluctuation base-level. *Sediment. Geol.* **1997**, *112*, 195–217. [https://doi.org/10.1016/S0037-0738\(97\)00035-3](https://doi.org/10.1016/S0037-0738(97)00035-3).
21. Cattaneo, A.; Steel, R. Transgressive deposits: A review of their variability. *Earth-Sci. Rev.* **2003**, *62*, 187–228. [https://doi.org/10.1016/S0012-8252\(02\)00134-4](https://doi.org/10.1016/S0012-8252(02)00134-4).
22. Lobo, F.J.; Ridente, D. Stratigraphic architecture and spatio-temporal variability of high frequency (Milankovitch) depositional cycles on modern continental margins: An overview. *Mar. Geol.* **2014**, *352*, 215–247. <https://doi.org/10.1016/j.margeo.2013.10.009>.
23. Posamentier, H.W.; Allen, G.P.; James, D.P.; Tesson, M. Forced regressions in a sequence stratigraphic framework: Concepts, examples, and exploration significance. *AAPG Bull.* **1992**, *76*, 1687–1709.
24. Catuneanu, O. Sequence stratigraphy of clastic systems: Concepts, merits, and pitfalls. *J. Afr. Earth Sci.* **2002**, *35*, 1–43. [https://doi.org/10.1016/S0899-5362\(02\)00004-0](https://doi.org/10.1016/S0899-5362(02)00004-0).
25. Bozzano, A.; Corradi, N.; Fanucci, F.; Ivaldi, R. Late Quaternary deposits from the Ligurian continental shelf (NW Mediterranean): A response to problems of coastal erosion. *Chem. Ecol.* **2006**, *22* (Suppl. 1), S349–S359. <https://doi.org/10.1080/02757540600688036>.
26. Sulli, A.; Agate, M.; Mancuso, M.; Pepe, F.; Pennino, V.; Polizzi, S.; Lo Presti, V.; Gargano, F.; Interbartolo, F. Variability of depositional setting along the north-western Sicily continental shelf (Italy) during Late Quaternary: Effects of sea level changes and tectonic evolution. *Alp. Mediterr. Quat* **2012**, *25*, 141–156.
27. Martorelli, E.; Falese, F.; Chiocci, F.L. Chapter 12 Overview of the variability of Late Quaternary continental shelf deposits of the Italian peninsula. In *Continental Shelves of the World: Their Evolution During the Last Glacio-Eustatic Cycle*, 1st ed.; Memoirs; Chiocci, F.L., Chivas, A.R., Eds.; Geological Society of London: London, UK, 2014; Volume 41, pp. 171–186. <https://doi.org/10.1144/M41.12>.
28. Aiello, G.; Budillon, F.; Cristofalo, G.; D’Argenio, B.; de Alteriis, G.; De Lauro, M.; Ferraro, L.; Marsella, E.; Pelosi, N.; Sacchi, M.; et al. Marine Geology and Morphobathymetry in the Bay of Naples (South-Eastern Tyrrhenian Sea, Italy). In *Mediterranean Ecosystems*, 1st ed.; Faranda, F.M., Guglielmo, L., Spezie, G., Eds.; Springer: Milano, Italy, 2001; pp. 1–8.
29. D’Argenio, B.; Aiello, G.; de Alteriis, G.; Milia, A.; Sacchi, M.; Tonielli, R.; Budillon, F.; Chiocci, F.L.; Conforti, A.; De Lauro, M.; et al. *Digital Elevation Model of the Naples Bay and adjacent areas, Eastern Tyrrhenian sea*, 1st ed.; Editore De Agostini: Rome, Italy, 2004; pp. 1–10.
30. Sacchi, M.; Insinga, D.D.; Milia, A.; Molisso, F.; Torrente, M.M.; Conforti, A. Stratigraphic signature of the Vesuvius 79 A.D. event off the Sarno prodelta system, Naples Bay. *Mar. Geol.* **2005**, *222*, 443–469. <https://doi.org/10.1016/j.margeo.2005.06.014>.
31. Insinga, D.D.; Molisso, F.; Lubritto, C.; Sacchi, M.; Passariello, I.; Morra, V. The proximal marine record of Somma–Vesuvius volcanic activity in the Naples and Salerno bays, Eastern Tyrrhenian Sea, during the last 3 kyrs. *J. Volcanol. Geotherm. Res.* **2008**, *177*, 170–186. <https://doi.org/10.1016/j.jvolgeores.2007.07.011>.
32. Savini, A.; Basso, D.; Bracchi, V.A.; Corselli, C.; Pennetta, M. Maërl-bed mapping and carbonate quantification on submerged terraces offshore the Cilento peninsula (Tyrrhenian Sea, Italy). *Geodiversitas* **2012**, *34*, 77–98. <https://doi.org/10.5252/g2012n1a5>.
33. Pennetta, M.; Bifulco, A.; Savini, A. Ricerca di depositi di sabbia sottomarina relitta sulla piattaforma continentale del Cilento (SA) utilizzabile per interventi di ripascimento artificiale dei litorali. *Geol. Dell’ambiente* **2013**, *1*, 1–22.
34. Savini, A.; Bracchi, V.A.; Cammarosano, A.; Pennetta, M.; Russo, F. Terraced landforms onshore and offshore the Cilento Promontory (south-eastern Tyrrhenian margin) and their significance as Quaternary records of sea level changes. *Water* **2021**, *13*, 566. <https://doi.org/10.3390/w13040566>.
35. Trenhaile, A.S. *The Geomorphology of Rocky Coasts*, 1st ed.; Oxford University Press: Oxford, UK, 1987; pp. 1–384. <https://doi.org/10.1177/030913338801200215>.
36. Retallack, G.J.; Roering, J.J. Wave-cut or water-table platforms of rocky coasts and rivers? *GSA Today* **2012**, *22*, 4–10. <https://doi.org/10.1130/GSATG144A.1>.
37. Guida, D.; Valente, A. Terrestrial and marine landforms along the Cilento coastland (Southern Italy): A framework for landslide hazard assessment and environmental conservation. *Water* **2019**, *11*, 2618. <https://doi.org/10.3390/w11122618>.
38. De Pippo, T.; Pennetta, M. Terrazzi deposizionali sommersi nel Golfo di Policastro (Campania). *Mem. Descr. Carta Geol.* **2004**, *LVIII*, 57–62.
39. Casalbore, D.; Romagnoli, C.; Adami, C.; Bosman, A.; Falese, F.; Ricchi, A.; Chiocci, F.L. Submarine depositional terraces at Salina island (Southern Tyrrhenian sea) and implications on the Late-Quaternary evolution of the insular shelf. *Geosciences* **2018**, *8*, 20. <https://doi.org/10.3390/geosciences8010020>.

40. Budillon, F.; Amodio, S.; Contestabile, P.; Alberico, I.; Innangi, S.; Molisso, F. *The Present-Day Nearshore Submarine Depositional Terraces off the Campania Coast (South-Eastern Tyrrhenian Sea): An Analysis of Their Morpho-Bathymetric Variability*; Extended Abstract; IMEKO TC-19 International Workshop on Metrology for the Sea: Naples, Italy, 2020; pp. 132–138.
41. Milia, A.; Torrente, M.M. Late-Quaternary volcanism and transtensional tectonics in the Bay of Naples, Campanian continental margin, Italy. *Mineral. Petrol.* **2003**, *79*, 49–65. <https://doi.org/10.1007/s00710-003-0001-9>.
42. Chiocci, F.L.; Chivas, A.L. Chapter 1 An overview of the continental shelves of the world. In *Continental Shelves of the World: Their Evolution during the Last Glacio-Eustatic Cycle*, 1st ed.; Chiocci, F.L., Chivas, A.R., Eds.; Memoirs; Geological Society of London: London, UK, 2014; Volume 41, pp. 1–5. <https://doi.org/10.1144/M41.1>.
43. Aiello, G.; Marsella, E. Interactions between Late Quaternary volcanic and sedimentary processes in the Naples Bay, Southern Tyrrhenian sea. *Ital. J. Geosci.* **2015**, *134*, 367–382. <https://doi.org/10.3301/IJG.2014.56>.
44. Bartole, R. Tectonic structure of the Latian-Campanian shelf (Tyrrhenian Sea). *Boll. Di Oceanol. Teor. Appl.* **1984**, *2*, 197–230.
45. Bartole, R.; Savelli, C.; Tramontana, M.; Wezel, F.C. Structural and sedimentary features in the Tyrrhenian margin off Campania, southern Italy. *Mar. Geol.* **1984**, *55*, 163–180. [https://doi.org/10.1016/0025-3227\(84\)90067-7](https://doi.org/10.1016/0025-3227(84)90067-7).
46. Aiello, G.; Di Fiore, V.; Marsella, E.; D'Isanto, C. Stratigrafia sismica e morfobatimetria della Valle di Salerno. In Proceedings of the 26th National Congress GNGTS (Gruppo Nazionale di Geofisica della Terra Solida), Rome, Italy, 2007; 24–27 November 2007, Extended Abstract, pp. 495–498.
47. Aiello, G.; Marsella, E.; Di Fiore, V.; D'Isanto, C. Stratigraphic and structural styles of half-graben offshore basins in Southern Italy: Multichannel seismic and Multibeam morpho-bathymetric evidences on the Salerno Valley (Southern Campania continental margin, Italy). *Quad. Geofis.* **2009**, *77*, 1–33.
48. Sacchi, M.; Infuso, S.; Marsella, E. Late Pliocene-early Pleistocene compressional tectonics in offshore Campania (eastern Tyrrhenian sea). *Boll. Geof. Teor. Appl.* **1994**, *36*, 469–482.
49. Aiello, G.; Marsella, E.; Cicchella, A.G.; Di Fiore, V. New insights on morpho-structures and seismic stratigraphy along the Campania continental margin (Southern Italy) based on deep multichannel seismic profiles. *Rend. Lincei* **2011**, *22*, 349–373.
50. Aiello, G.; Cicchella, A.G. Dati sismostratigrafici sul margine continentale della Campania tra Ischia, Capri ed il Bacino del Volturno (Tirreno meridionale, Italia) in base al processing sismico ed all'interpretazione geologica di profili sismici a riflessione multicanale. *Quad. Geof.* **2019**, *149*, 1–52.
51. Zitellini, N.; Ranero, C.; Loreto, M.F.; Ligi, M.; Pastore, M.; D'Oriano, F.; Sallares, V.; Grevemeyer, I.; Moeller, S.; Prada, M. Recent inversion of the Tyrrhenian Basin. *Geology* **2020**, *48*, 123–127. <https://doi.org/10.1130/G46774.1>.
52. Bonardi, G.; Amore, F.O.; Ciampo, G.; De Capoa, P.; Miconnet, P.; Perrone, V. Il Complesso Liguride Auct: Stato delle conoscenze e problemi aperti sull'evoluzione pre-appenninica ed i suoi rapporti con l'Arco Calabro. *Mem. Soc. Geol. Ital.* **1988**, *41*, 17–35.
53. Cammarosano, A.; Cavuoto, G.; Martelli, L.; Nardi, G.; Toccaceli, R.M.; Valente, A. Il Progetto CARG nell'area silentina (area interna Appennino meridionale): Il nuovo assetto stratigrafico-strutturale derivante dal rilevamento dei fogli 503, 502, e519 (Vallo della Lucania, Agropoli e Capo Palinuro). *Rend. Online Soc. Geol. Ital.* **2011**, *12*, 19–21.
54. Vitale, S.; Ciarcia, S. Tectono-stratigraphic setting of the Campania region (southern Italy). *J. Maps* **2018**, *14*, 9–21. <https://doi.org/10.1080/17445647.2018.1424655>.
55. Gasperini, L.; Stanghellini, G. SEISPRHO: An interactive computer program for processing and interpretation of high-resolution seismic reflection profiles. *Comp. and Geosci.* **2009**, *35*, 1497–1507. <https://doi.org/10.1016/j.cageo.2008.04.014>.
56. Vail, P.R.; Hardenbol, J.; Todd, R.G. Jurassic unconformities, chronostratigraphy, and sea-level changes from seismic stratigraphy and biostratigraphy. In *Interregional Unconformities and Hydrocarbon Accumulation*, 1st ed.; Memoirs; Schlee, J.S., Ed.; American Association of Petroleum Geologists: Tulsa, OK, USA, 1984; Volume 36, pp. 129–144.
57. Ferraro, L.; Pescatore, T.; Russo, B.; Senatore, M.R.; Vecchione, C.; Coppa, M.G.; Di Tuoro, A. Studi di geologia marina del margine tirrenico: La piattaforma continentale tra Punta Licosa e Capo Palinuro (Tirreno meridionale). *Boll. Soc. Geol. Ital.* **1997**, *116*, 473–485.
58. Shackleton, N.J.; Opdyke, N.D. Oxygen isotope and paleomagnetic stratigraphy of equatorial Pacific Core V28-238: Oxygen isotope temperatures and ice volume on a 105 year and 106 year scale. *Quat. Res.* **1973**, *3*, 39–55. [https://doi.org/10.1016/0033-5894\(73\)90052-5](https://doi.org/10.1016/0033-5894(73)90052-5).
59. Zazo, C. Interglacial sea levels. *Quat. Intern.*, **1999**, *55* (1), 101–113. [https://doi.org/10.1016/S1040-6182\(98\)00031-7](https://doi.org/10.1016/S1040-6182(98)00031-7).
60. Emery, K.O. Relict Sediments on Continental Shelves of World. *AAPG Bull.* **1968**, *52*, 445–464.
61. Swift, D.J.P. Continental shelf sedimentation. In *Marine Sediment Transport and Environmental Management*, 1st ed.; Stanley, D.J., Swift, D.J.P., Eds.; John Wiley: New York, NY, USA, 1976; pp. 311–350.
62. Orme, G.R. Relict sediment. In *Beaches and Coastal Geology. Encyclopedia of Earth Sciences Series*; Springer: New York, NY, USA, 1982; https://doi.org/10.1007/0-387-30843-1_362.
63. Péres, J.M.; Picard, J. Nouveau manuel de bionomie marine benthique de la Mer Méditerranée. *Recl. Trav. Stn. Mar. D'endoume* **1964**, *31* (47), 5–137.
64. Thorne, J.A.; Swift, D.J.P. Sedimentation on continental margins: VI. A regime model for depositional sequences, their component systems tracts, and bounding surfaces. In *Shelf Sand and Sandstone Bodies—Geometry, Facies and Sequence Stratigraphy*, 1st ed.; Swift, D.J.P., Oertel, G.F., Tillman, R.W., Thorne, J.A., Eds.; Special Publication; International Association of Sedimentologists, Wiley: New York, NY, USA, 1991; Volume 14, pp. 189–255. <https://doi.org/10.1002/9781444303933.ch2>.

65. Carannante, G.; Esteban, M.; Milliman, J.D.; Simone, L. Carbonate lithofacies as a paleolatitude indicators: Problems and limitations. *Sedim. Geol.* **1988**, *60*, 333–346. [https://doi.org/10.1016/0037-0738\(88\)90128-5](https://doi.org/10.1016/0037-0738(88)90128-5).
66. Ruddiman, W.F.; McIntyre, A. The mode and mechanism of the last deglaciation: Oceanic evidence. *Quat. Res.* **1981**, *16*, 125–134. [https://doi.org/10.1016/0033-5894\(81\)90040-5](https://doi.org/10.1016/0033-5894(81)90040-5).
67. Jansen, E.; Overpeck, J.; Briffa, K.R.; Duplessy, J.C.; Joos, F.; Masson-Delmotte, V.; Olago, D.; Otto-Bliesner, B.; Peltier, W.R.; Rahmstorf, S.; et al. Palaeoclimate. In *Climate Change: The Physical Science Basis. Contribution of Working Group I to the Fourth Assessment Report of the Intergovernmental Panel on Climate Change*; Solomon, S., Qin, D., Manning, M., Chen, Z., Marquis, M., Averyt, K.B., Tignor, M., Miller, H.L., Eds.; Cambridge University Press: Cambridge, UK; New York, NY, USA, 2007.
68. Ruddiman, W.F. The early anthropogenic hypothesis: Challenges and responses. *Rev. Geophys.* **2007**, *45*, RG4001. <https://doi.org/10.1029/2006RG000207>.
69. Murray-Wallace, C.; Woodroffe, C.D. Sea-level changes since the Last Glacial Maximum. In *Quaternary Sea-Level Changes: A Global Perspective*, 1st ed.; Murray-Wallace, C., Woodroffe, C.D., Eds.; Cambridge University Press: Cambridge, UK, 2014; pp. 320–368.
70. Fairbridge, R.W. Eustatic changes in sea level. *Phys. Chem. Earth* **1961**, *4*, 99–185. [https://doi.org/10.1016/0079-1946\(61\)90004-0](https://doi.org/10.1016/0079-1946(61)90004-0).
71. Fairbanks, R.G. A 17,000-year glacio-eustatic sea level record: Influence of glacial melting rates on the Younger Dryas event and deep-ocean circulation. *Nature* **1989**, *342*, 637–642. <https://doi.org/10.1038/342637a0>.
72. Varekamp, J.C.; Thomas, E.; Van de Plassche, O. Relative sea-level rise and climate change over the last 1500 years. *Terra Nova* **1992**, *4*, 293–304. <https://doi.org/10.1111/j.1365-3121.1992.tb00818.x>.
73. Benjamin, J.; Rovere, A.; Fontana, A.; Furlani, S.; Vacchi, M.; Inglis, R.H.; Galili, E.; Antonioli, F.; Sivan, D.; Miko, S.; et al. Late Quaternary sea-level changes and early human societies in the central and eastern Mediterranean Basin: An interdisciplinary review. *Quat. Int.* **2017**, *449*, 29–57. <https://doi.org/10.1016/j.quaint.2017.06.025>.
74. Antonioli, F.; De Falco, G.; Lo Presti, V.; Moretti, L.; Scardino, G.; Anzidei, M.; Bonaldo, D.; Carniel, S.; Leoni, G.; Furlani, S.; et al. Relative Sea-Level Rise and Potential Submersion Risk for 2100 on 16 Coastal Plains of the Mediterranean Sea. *Water* **2020**, *12*, 2173. <https://doi.org/10.3390/w12082173>.
75. Chiocci, F.L.; D'Angelo, S.; Orlando, L.; Pantaleone, E.A. Evolution of the Holocene shelf sedimentation defined by high-resolution seismic stratigraphy and sequence analysis (Calabro-tyrrhenian continental shelf). *Mem. Soc. Geol. Ital.* **1989**, *48*, 359–380.
76. Díaz, J.I.; Maldonado, A. Transgressive sand bodies on the Maresme continental-shelf, western Mediterranean-sea. *Mar. Geol.* **1990**, *91*, 53–72.
77. Trincardi, F.; Campiani, E.; Correggiari, A.; Fogliani, F.; Maselli, V.; Remia, A. Bathymetry of the Adriatic Sea: The legacy of the last eustatic cycle and the impact of modern sediment dispersal. *Journ. of Maps*, **2014**, *10* (1), 151–158. <https://doi.org/10.1080/17445647.2013.864844>
78. Ercilla, G.; Estrada, F.; Casas, D.; Duran, R.; Nuez, M.; Alonso, B.; Farran, M.L. The El Masnou infralittoral sedimentary environment (Barcelona province, NW Mediterranean Sea): Morphology and Holocene seismic stratigraphy. *Sci. Mar.* **2010**, *74*, 179–196. <https://doi.org/10.3989/scimar.2010.74n1179>.
79. Ridente, D. Late Pleistocene Post-Glacial Sea Level Rise and Differential Preservation of Transgressive “Sand Ridge” Deposits in the Adriatic Sea. *Geosciences* **2018**, *8*, 61. <https://doi.org/10.3390/geosciences8020061>.
80. Distefano, S.; Gamberi, F.; Baldassini, N.; Di Stefano, A. Quaternary Evolution of Coastal Plain in Response to Sea-Level Changes: Example from South-East Sicily (Southern Italy). *Water* **2021**, *13*, 1524. <https://doi.org/10.3390/w13111524>.
81. Bonifay, E. L'Ere Quaternaire: Definition, limites and subdivision sur la base de la chronologie mediterraneenne. *Bull. Soc. Geol. Fr.* **1975**, *17*, 380–393.
82. Yokoyama, Y.; Purcell, A. On the geophysical processes impacting palaeo-sea-level observations. *Geosci. Lett.* **8**, 13 (2021). <https://doi.org/10.1186/s40562-021-00184-w>.
83. Lambeck, K.; Yokoyama, Y.; Purcell, T. Into and out of the Last Glacial Maximum: Sea-level change during Oxygen Isotope Stages 3 and 2. *Quat. Sci. Rev.* **2002**, *21*, 343–360. [https://doi.org/10.1016/S0277-3791\(01\)00071-3](https://doi.org/10.1016/S0277-3791(01)00071-3).
84. Lambeck, K.; Antonioli, F.; Purcell, A.; Silenzi, S. Sea-level change along the Italian coast for the past 10,000 yr. *Quat. Sci. Rev.* **2004**, *23*, 1567–1598. <https://doi.org/10.1016/j.quascirev.2004.02.009>.
85. Ferranti, L.; Antonioli, F.; Mauz, B.; Amorosi, A.; Dai Pra, G.; Mastronuzzi, G.; Monaco, C.; Orrù, P.; Pappalardo, M.; Radtke, U.; et al. Markers of the last interglacial sea-level high stand along the coast of Italy: Tectonic implications. *Quat. Int.* **2006**, *145–146*, 30–54. <https://doi.org/10.1016/j.quaint.2005.07.009>.
86. Peltier, W.R.; Fairbanks, R.G. Global glacial ice volume and Last Glacial Maximum duration from an extended Barbados sea level record. *Quat. Sci. Rev.* **2006**, *25*, 3322–3337. <https://doi.org/10.1016/j.quascirev.2006.04.010>.
87. Lambeck, K.; Antonioli, F.; Anzidei, M.; Ferranti, L.; Leoni, G.; Scicchitano, G.; Silenzi, S. Sea level change along the Italian coast during the Holocene and projections for the future. *Quat. Int.* **2011**, *232*, 250–257. <https://doi.org/10.1016/j.quaint.2010.04.026>.
88. Ishiwa, T.; Yokoyama, Y.; Okuno, J.; Obrochta, S.; Uehara, K.; Ikehara, M.; Miyairi, Y. A sea-level plateau preceding the Marine Isotope Stage 2 minima revealed by Australian sediments. *Sci. Rep.* **2019**, *9*, 6449. <https://doi.org/10.1038/s41598-019-42573-4>.
89. Cerrone, C.; Vacchi, M.; Fontana, A.; Rovere, A. Last Interglacial sea-level proxies in the Western Mediterranean. *Earth Syst. Sci. Data Discuss.* **2021**, *13*, 4485–4527. <https://doi.org/10.5194/essd-2021-49>.
90. Thompson, S.B.; Creveling, J.R. A Global Database of Marine Isotope Stage 5a and 5c Marine Terraces and Paleoshoreline Indicators. *Earth Syst. Sci. Data Discuss.* **2021**, *13*, 3467–3490. <https://doi.org/10.5194/essd-2021-14>.

91. Mitchum, R.M. Seismic stratigraphy and global changes of sea level. Part 11: Glossary of terms used in seismic stratigraphy. In *Seismic Stratigraphy—Applications to Hydrocarbon Exploration*, 1st ed.; Payton, C.E., Ed.; Memoirs; American Association Petroleum Geologists: Tulsa, OK, USA, 1977; Volume 26, pp. 205–212.
92. Hunt, D.; Tucker, M.E. Stranded parasequences and the forced regressive wedge systems Tract: Deposition during base-level fall. *Sedim. Geol.* **1992**, *81*, 1–9.
93. Posamentier, H.W.; Allen, G.P. Siliciclastic Sequence Stratigraphy: Concepts and applications. *SEPM Concepts Sedimentol. Paleontol.* **1999**, *7*, 1–210. <https://doi.org/10.1029/EO082i013p00156>.
94. Plint, A.G.; Nummedal, D. The Falling Stage Systems Tract: Recognition and importance in sequence stratigraphic analysis. In *Sedimentary Response to Forced Regression*, 1st ed.; Hunt, D., Gawthorpe, R.L., Eds.; Special Publication; Geological Society of London: London, UK, **2000**; Volume 172, pp. 1–17. <https://doi.org/10.1144/GSL.SP.2000.172.01.01>.